

Research Article

Numerical Study of Stresses around Holes Drilled and Filled by Expansive Cement: Case of Isotropic Linear Elastic Block of Rock

Mambou Ngueyep Luc Leroy ^{1,2} and Gael Nkenwoum Chebou²

¹School of Geology and Mining Engineering, University of Ngaoundéré, P.O. Box 115, Ngaoundéré, Cameroon

²Laboratory of Material Sciences, Department of Physics, Faculty of Sciences, University of Yaoundé 1, P.O. Box 812, Yaoundé, Cameroon

Correspondence should be addressed to Mambou Ngueyep Luc Leroy; mamboulucroy@gmail.com

Received 31 March 2018; Revised 20 May 2018; Accepted 24 May 2018; Published 21 June 2018

Academic Editor: Jose Cesar de Sa

Copyright © 2018 Mambou Ngueyep Luc Leroy and Gael Nkenwoum Chebou. This is an open access article distributed under the Creative Commons Attribution License, which permits unrestricted use, distribution, and reproduction in any medium, provided the original work is properly cited.

This work dealt with an essential problem of fragmentation of rocks with expansive cement. The redistribution and magnitude of stresses and displacement generated around holes were done by using Ansys Inc. Code which is based on finite element code. Blocks of rock with one hole, two holes, and nine holes drilled in square mesh and staggered mesh have been considered. Numerical results reveal that many factors can influence the mechanism of fragmentation of a rock by using expansive cement: hole diameter, hole spacing, panel mesh, expansive pressure applied, and the elastic properties of the massif. Stresses and displacements generated globally decrease when spacing holes increase. Normal stresses allow a better stress interaction between holes in the case of square mesh disposition. Staggered mesh disposition generates higher stresses than the square mesh disposition. But the square mesh disposition can be useful for controlled fragmentation in order to obtain block of rock with square geometry. For each expansive cement and rock, there exist suitable range of diameter and spacing hole which can generate high stresses for breaking the rock.

1. Introduction

Explosives play a leading role in modern industries. They are used for the extraction of metals; industrial minerals; mineral exploration works; or the construction of roads, railways, or hydroelectric plants. The excavation and fragmentation with explosives is an integral part of the technology mostly used by man to excavate the rock for multiple uses. However, the blasting is also accompanied by air pollution, noise pollution, alteration of soil, and fauna and flora, as well as social problems due to conflicts of interest, home transfers, and so on.

Due to the environmental and social impact related to blasting of rocks, new methods of fragmentation have been developed including the expansive cement fracturing.

Nonexplosive fracturing of rocks is one of the main rock-breaking methods in hard rock quarries or for the demolition of any concrete structure and is usually accomplished through

the use of nonexplosive expansion material (NEEM). Although this method of rock breaking is without noise or vibrations and the entire operation is controllable, safe, and easy, the process is lengthier compared to the blasting method. “Expansive cements are inorganic binders that generate expansive stresses in the hardened paste in the course of hydration, counteracting the tensile stresses generated by chemical shrinkage and drying shrinkage.” [1]. This method consists of introducing expansive cement into previously drilled holes, and the expansive stresses created by the cement will have the function of initiating cracks and spreading them over the entire massif. Many studies experimentally showed that expansive cement is capable of breaking rocks [2–4]. However, evaluation and knowledge of stresses which occur around the hole become very important to control fragmentation. Many models have been established to analytically and numerically simulate the cracks, stress, and strain around the hole.

In 1987 and 1992, Aifantis [5–7] introduced the theory of gradient elastic and it has been used successfully for predicting shear band widths and spacings, as well as for eliminating strain singularities from dislocation lines and elastic crack tips. In 2003, Mastorakos et al. [8] simulated the discrete crack propagation. Their study showed that there is a characteristic relation between critical stress and crack growth for different initial defect concentrations. Moreover, the crack path is of a fractal character, and the crack velocity dependence on the stress intensity factor follows a power law relationship, in accordance with experimental trends.

In 2004, Efreimidis et al. [9] used a simplified gradient elasticity theory to analytically simulate the behavior of the hollow cylinder loaded by internal and external pressure. It follows that gradient theory in its simplest form is able to capture the size effect in contrast with elasticity theory. In 2009, Aifantis [10] also used a gradient approach to predict a significant size effect: smaller holes experience lower stress concentration factors in accordance with intuition; in addition, he showed that micropolar theory gives measurable effects only for specimens with very small hole sizes and couple stress theory gives measurable effects only for small and medium size holes.

Recently in 2016, Bagni et al. [11] proposed a new approach based on the combination of the Ru–Aifantis theory of gradient elasticity and the theory of critical distances (TCD) for the fatigue assessment of notched metallic components. The proposed methodology represents an important step forward respect to the state of the art, allowing an accurate fatigue assessment of engineering components, by postprocessing the relevant gradient-enriched stresses directly on the surface of the component, with evident advantages from a practical point of view. Also in 2016, Aifantis [12] investigated internal length gradient (ILG) material mechanics across scales and disciplines. In their study, three apparently different emerging research areas of current scientific/technological/biomedical interest are discussed: (i) plastic instabilities and size effects in nanocrystalline (NC)/ultrafine grain (UFG) and bulk metallic glass (BMG) materials; (ii) chemomechanical damage, electromechanical degradation, and photomechanical aging in energetic materials; (iii) brain tissue and neural cell modeling. All these cited studies are based on the theory of gradient elastic, gradient plasticity, gradient chemomechanics, and gradient electromechanics. However, based on the theory of classic elastic linear behavior of rock, the analytical numerical solutions and of stresses redistribution were proposed by many researchers. Timoshenko and Goodier proposed the analytical calculation of stress redistribution around a circular hole [5]. Arshadnejad et al. used Timoshenko and Goodier's theory of plasticity to determine the redistribution of stress between two circular holes [13]. In 2009, Arshadnejad et al. used phase 2 code based on finite elements to study numerically the redistribution of stresses between two circular holes [13].

In 2011, Arshadnejad et al. [14] developed an empirical model based on hole spacing to determine the pressure of NEEM in the rock fracture process. Primarily, the empirical model was developed by the mathematical method, using

dimensional analysis. Then, the phase code, which is based on the finite element method, was utilized to predict growth of crack in rocks. The results of numerical analysis show slight deviations from the empirical model.

In 2012, Sburlati [15] obtained analytical solutions for thick-walled cylinders subjected to internal and external pressures in which the entire wall is made of functionally graded material or of only a thin functionally graded coating present on the internal homogeneous wall. This investigation permitted to optimize the elastic response of cylinders under pressure by tailoring the thickness variation of the elastic properties and to reduce manufacturing costs given by the technological limitations that occur to produce entire functionally graded walls.

In 2017, Shen et al. [16] investigated a new simple mathematical method to predict rock stress around a non-circular tunnel, and the method is calibrated and validated with a numerical model. It can be found that the tunnel shapes and polar angles affect the applicable zone of the theoretical model significantly, and the applicable zone of a rectangular tunnel was obtained using this method.

Recently in 2018, Nkene et al. [17] studied analytically and numerically strain fields, stress fields, and displacements in a rotating hollow cylinder, whose walls were completely made in functionally graded materials (FGM). Their results showed that tangential stress, tangential strain, and displacements are higher at the inner surface and internal radial pressure strongly affects the radial stresses and radial strain.

However, to the best of our knowledge, the numerical analysis of the redistribution of stresses and displacement around a block of rock with more than two holes in the case of an isotropic system remains unaddressed. The effect of holes disposition is also investigated.

In this work, we used Ansys Inc. software for numerical analysis of stress redistribution and displacement by the application of expansive cement. This study concerns an isotropic elastic block with one hole, two holes, and nine holes drilled with disposition in the square mesh and staggered mesh. Ansys Inc. software is based on the finite element method. It is used to model complex behaviors and offers the best results. This enables us to observe in two or in three dimensions the redistribution and magnitude of stress, strain, and displacement in the medium.

This document is organized as follows. The finite element method based on the Rayleigh–Ritz method used is set out in Section 2. Section 3 is devoted to numerical simulations of the state of stress and displacement around a one, two, or nine circular hole(s) panel. Finally, the conclusion is given in Section 4.

2. Methods

2.1. The Distribution of Stress Field around a Circular Hole.

Let us consider a hollow cylinder with inner radius a and outer radius b under an axisymmetric radial loading (internal and external pressure loading, resp., P_i and P_o), as show in Figure 1. The distribution of stresses around a cylindrical hole with uniform loads inside and outside can be written in the following way [2]:

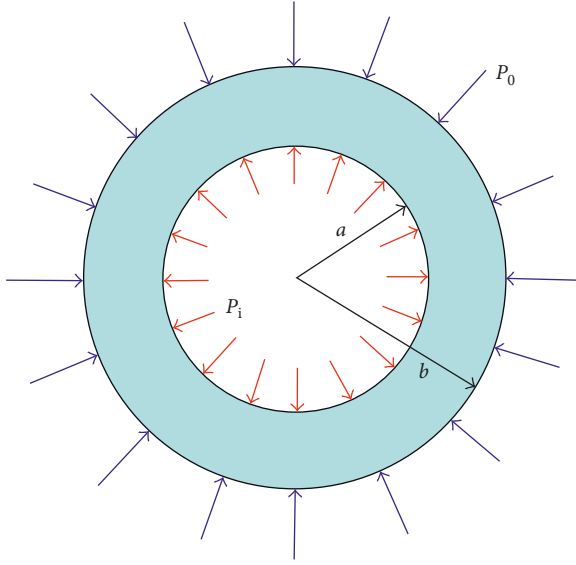


FIGURE 1: Distribution of stresses around a hollow cylinder.

$$\sigma_r = \frac{(a^2 p_i - b^2 p_0)}{b^2 - a^2} + \frac{a^2 b^2 (p_i - p_0)}{r^2 (b^2 - a^2)}, \quad (1)$$

$$\sigma_\theta = \frac{(a^2 p_i - b^2 p_0)}{b^2 - a^2} - \frac{a^2 b^2 (p_i - p_0)}{r^2 (b^2 - a^2)},$$

where σ_r and σ_θ are, respectively, the radial and tangential stresses; r is the distance between the center of the hole and the point considered; and p_i and p_0 are, respectively, the internal and external pressures applied on the hole. The distances a and b are, respectively, the internal and external radii of the cylinder.

If we consider a block with one hole drilled and filled with expansive cement, the expansive cement will develop a pressure noted p_i as shown in Figure 1. In the context of the use of expansive cement, the external pressure is zero and we only consider the internal pressure. The equation thus becomes [5]

$$\sigma_r = \frac{a^2 p_i}{b^2 - a^2} \left(1 + \frac{b^2}{r^2} \right), \quad (2)$$

$$\sigma_\theta = \frac{a^2 p_i}{b^2 - a^2} \left(1 - \frac{b^2}{r^2} \right).$$

And if we consider the outer radius b is very thick, we can reduce the equations again by tending b to infinity. So, we have [5]

$$\lim_{b \rightarrow \infty} \sigma_r = \frac{a^2 p_i}{r^2}, \quad (3)$$

$$\lim_{b \rightarrow \infty} \sigma_\theta = -\frac{a^2 p_i}{r^2}.$$

2.2. Redistribution of Stresses between Two Holes. Let us consider a block with two circular holes drilled and filled by

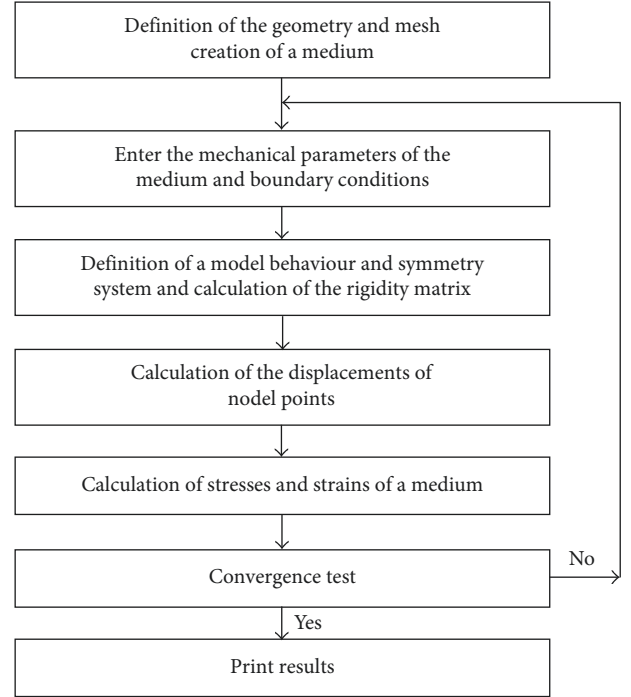


FIGURE 2: Algorithm of finite elements in linear elasticity [22].

expansive cement. These two holes are spaced to d and have a radius of r . According to the hole spacing, the stresses generate around the hole can interact. The equation of tangential and normal stresses around two holes becomes [5]

$$\sigma_r = C_r p_i \left(\frac{d}{2r} \right)^2, \quad (4)$$

$$\sigma_\theta = -C_\theta p_i \left(\frac{d}{2r} \right)^2,$$

where C_r and C_θ are the concentration factors of the radial and tangential stresses, respectively; d is the distance between holes; and r is the radius of holes.

In the case of a block with more than three holes, analytical resolutions become very complex, and therefore, the numerical method should be used. It is used to model complex behaviors and offers the best results. The finite element method is a numerical approximation method of solutions of partial differential equations [18, 19]. We use the Rayleigh–Ritz method [20, 21] based on the principle of minimum potential energy to establish the displacement equation of the medium as a function of the applied external forces. The general equation of displacement of nodes as function of force applied on nodes is given by

$$[K]\mathbf{q} = \mathbf{F}, \quad (5)$$

where \mathbf{q} is the global displacement vector, \mathbf{F} is the global vector of the loads applied on the nodes, and K is the rigidity matrix.

The algorithm based on the finite element method for solving our problems is shown in Figure 2:

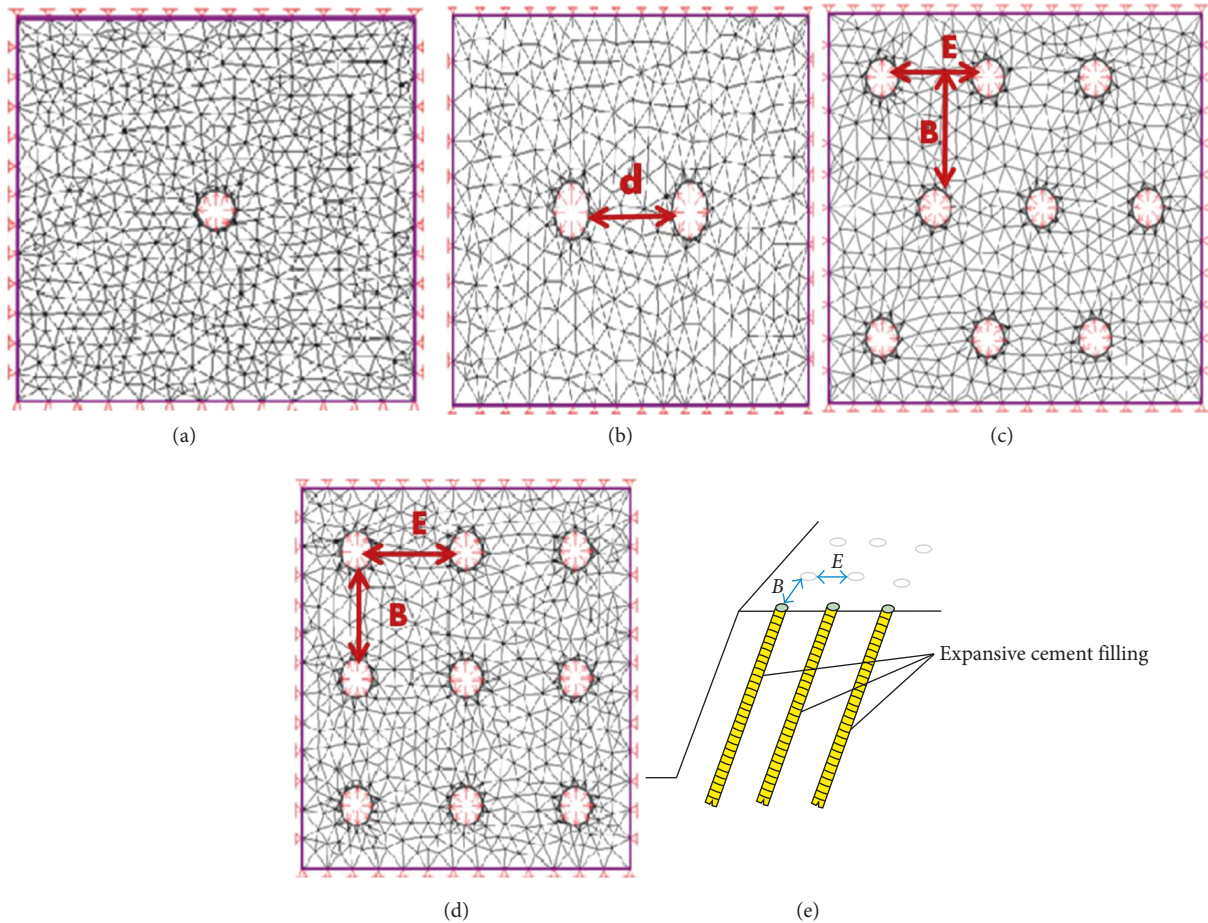


FIGURE 3: Presentation of the models studied.

This algorithm is valid for materials showing an isotropic or anisotropic linear elastic behavior because the elastic constants remain constant throughout the loading.

3. Numerical Analysis

3.1. Presentation of Models. The parameters of the material used for this numerical analysis are the density D , Young's modulus E , and Poisson's ratio ν . The material of our model is a granite block presenting an isotropic elastic behavior whose mechanical characteristics are [21] $D=2.75 \text{ g/cm}^3$, $E=50 \text{ GPa}$, and $\nu=0.1$. We have chosen granite rock because it is mostly exploited in quarry rock and mostly used in civil engineering. In the case of hard rocks (brittle material), the material is considered to behave in a linear elastic model.

The expansive cement used in this work is SPLITSTAR cement. It is mostly used in the demolition of rocks [14]. This cement is mainly composed of CaO. Its minimum pressure developed is 15 MPa [14]. We consider the minimum pressure in our numerical analysis with respect to the linear elastic model.

The meshing of our system is generated with a triangular mesh, and in order to have a better approximation of the results, the mesh density is more concentrated around the hole. Figure 3 presents the models used with the application

of 15 MPa pressure inside each hole (Figure 3). The initial conditions are

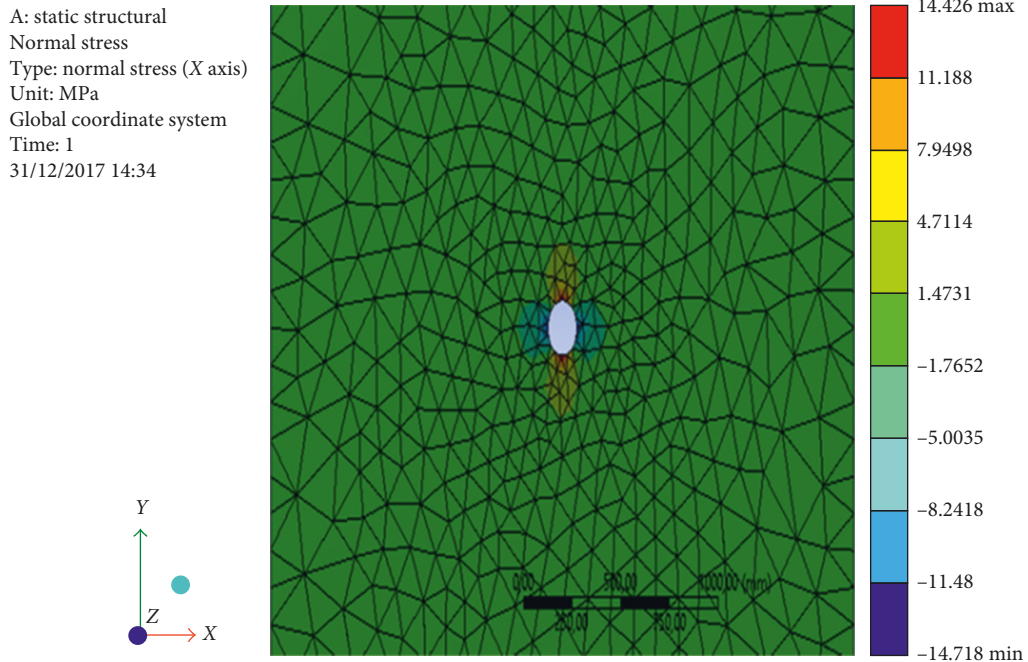
- (i) one degree of freedom,
- (ii) in situ stress neglected.

Figure 3(a) shows a panel with one hole with a diameter of 15 cm drilled in the block of 150 cm of side. Figure 3(b) shows a panel with two holes. It is a rectangle with a width of 100 cm and length of 150 cm. The diameter of the holes is 15 cm. The spacing between the holes is 50 cm. Figure 3(c) shows a nine-hole square-mesh panel. It is a square with a side of 150 cm. The diameter of the holes is 15 cm. The spaces between the holes of the same row are 50 cm, and the spacing between the rows is 50 cm. Figure 3(d) shows a panel with nine-hole-staggered mesh. It is a rectangle with a width of 150 cm and a length of 175 cm.

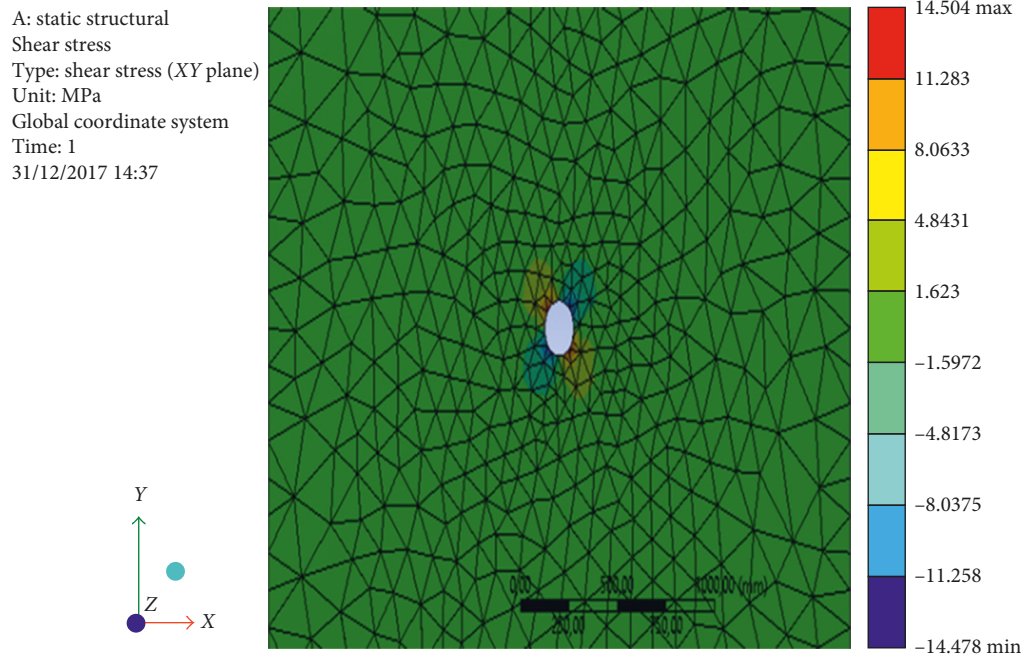
The diameter of the holes is 15 cm. The spacing between the holes of the same rows is 50 cm, and the spacing between the rows is 50 cm.

3.2. Numerical Result of the Redistribution of Stresses and Displacements around Circular Excavations

3.2.1. Case of a One-Hole Panel. Redistribution and magnitude of normal stress and shear stress around a hole drilled in an isotropic elastic block of rock are shown in Figure 4.



(a)



(b)

FIGURE 4: Redistribution of (a) normal stresses and (b) tangential stress.

In Figure 4, the parts of the excavation colored blue and red, respectively, represent the areas of compression and tension. As it is usual in rock mechanics, the negative sign stress values represent the compression stresses, while the positive sign represents the tension stresses. The respective maximum stresses are 14.426 MPa and 14.504 MPa, respectively, for normal stress and shear stress.

Figure 5 displays the surface isovalues of displacements.

Figure 5 shows the displacement of nodes around a circular excavation. The maximum displacements are located around the hole with a value of 0.024801 mm. These magnitudes of displacements are decreasing as one moves away from the hole due to the decrease in the stresses.

In Figure 6, it is noted that from $d = 15$ cm to 35 cm, normal stress and shear stress increase. The maximum

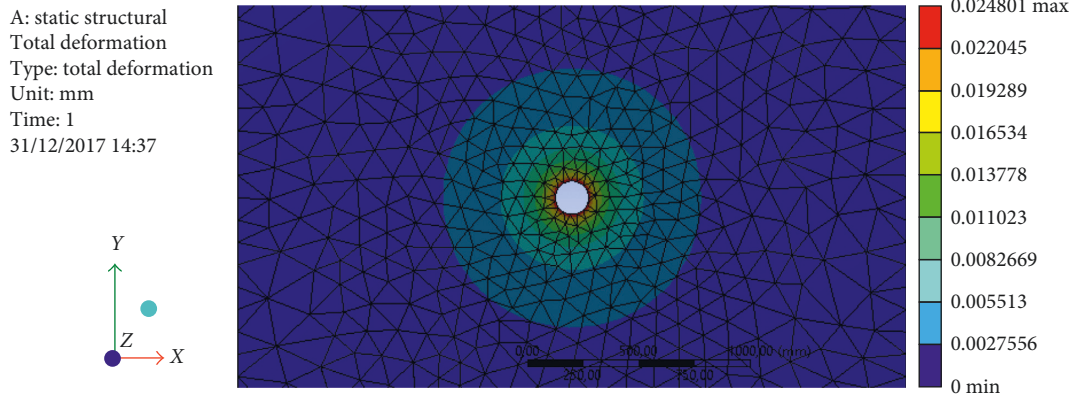


FIGURE 5: Redistribution of displacement.

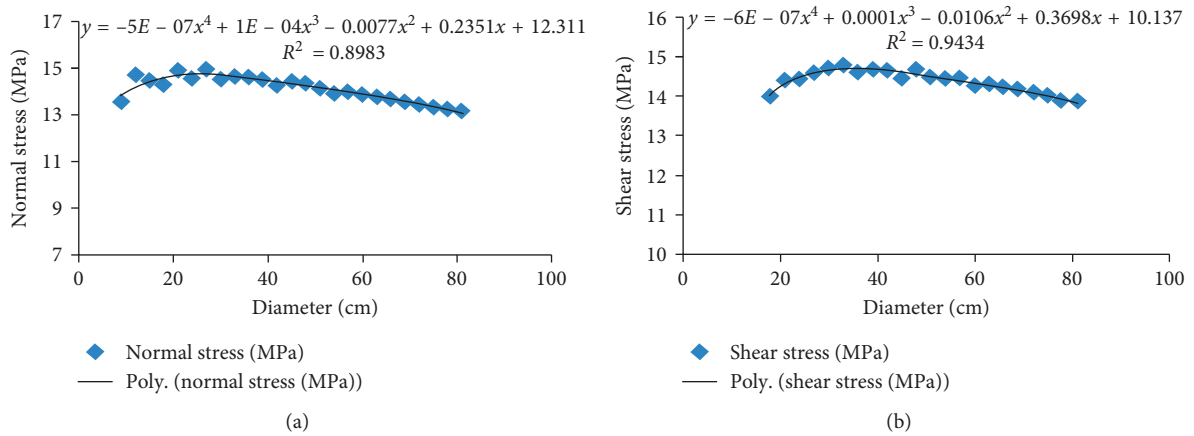


FIGURE 6: (a) Normal stress versus diameter of the hole. (b) Tangential stress versus diameter of the hole.

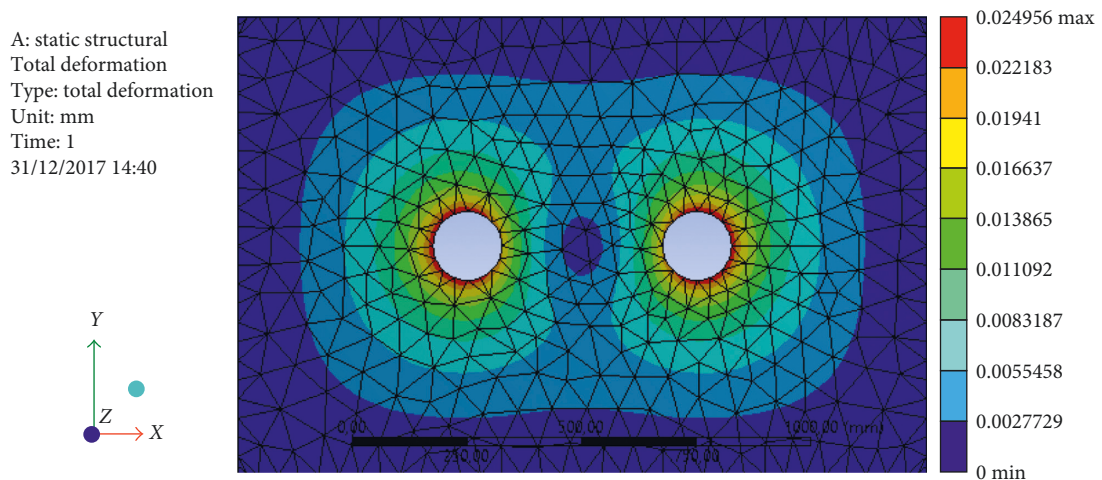
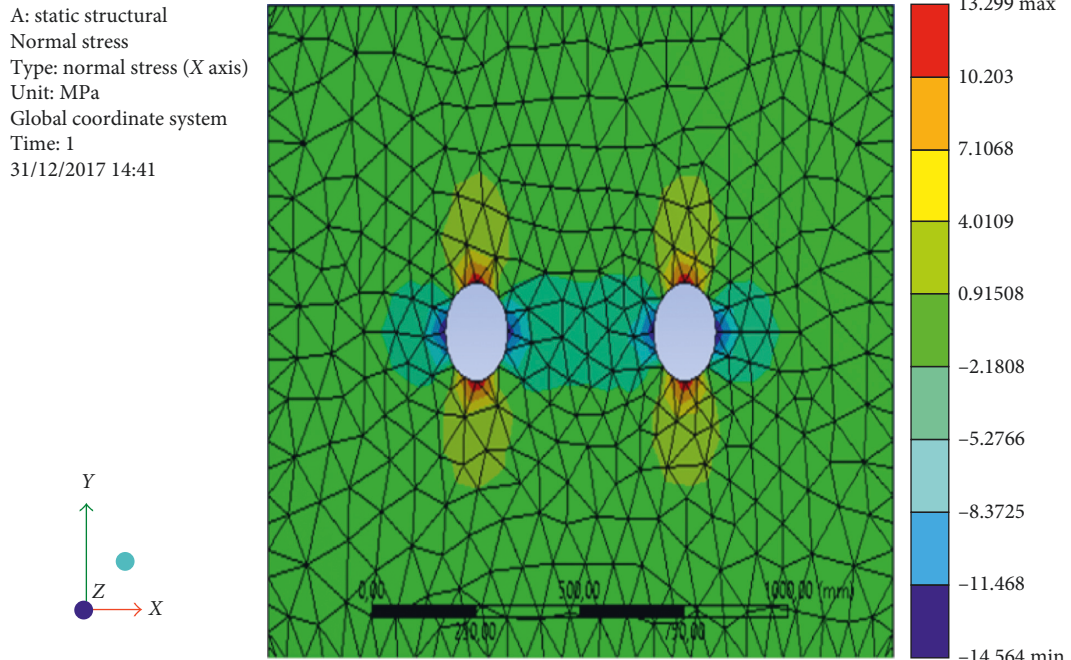


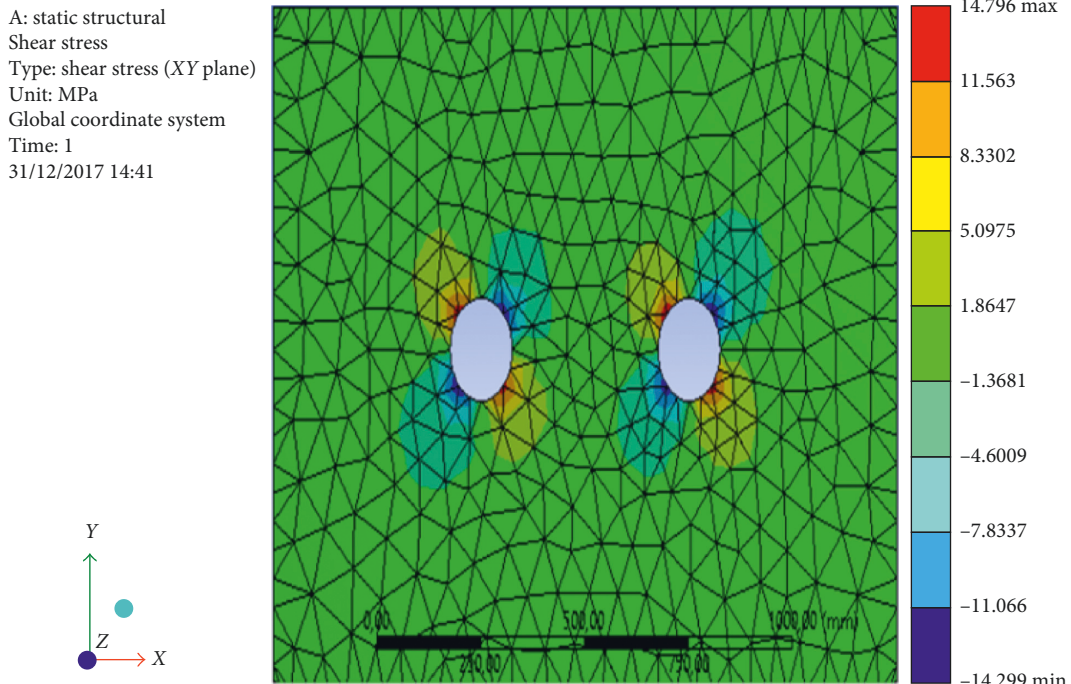
FIGURE 7: Redistribution of displacements.

stresses are obtained for $d = 35$ cm. For this granite rock and for an internal pressure of 15 MPa, the diameter of the hole is suitable for generating the high stresses which can break the rock. These results can be very useful for a mining engineer.

Above 35 cm of hole's diameter, the stresses generated decrease and cannot break the rock. In addition, the increase in the diameter of holes increases the consumption of expansive cement.



(a)



(b)

FIGURE 8: Redistribution of (a) normal stress and (b) tangential stress.

3.2.2. Case of Block with Two Holes. Hole spacing is the main parameter when the expansive cement is applied in drill holes to cause rock fracture.

Figures 7 and 8 present the redistribution and magnitude of the displacements and stresses around two circular holes filled by expansive cement.

In Figure 7, the maximum value of displacement is 0.024956 mm. It can be observed that there is interaction between the holes which allows the widening of the field of displacements. When the spacing hole increases, the intensity of the displacement decreases. The similar results were observed in [8, 9].

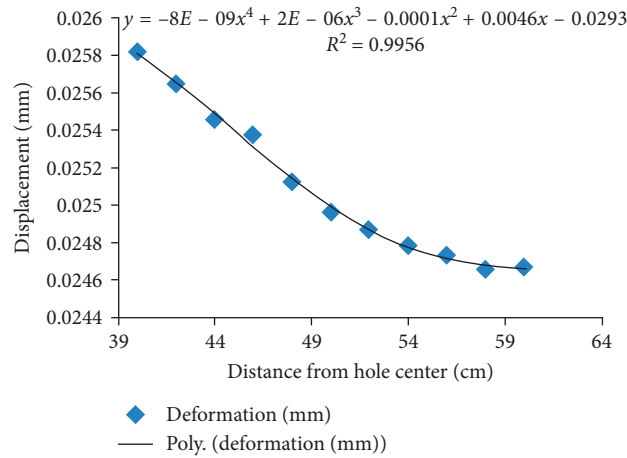


FIGURE 9: Displacement versus distance from the hole center.

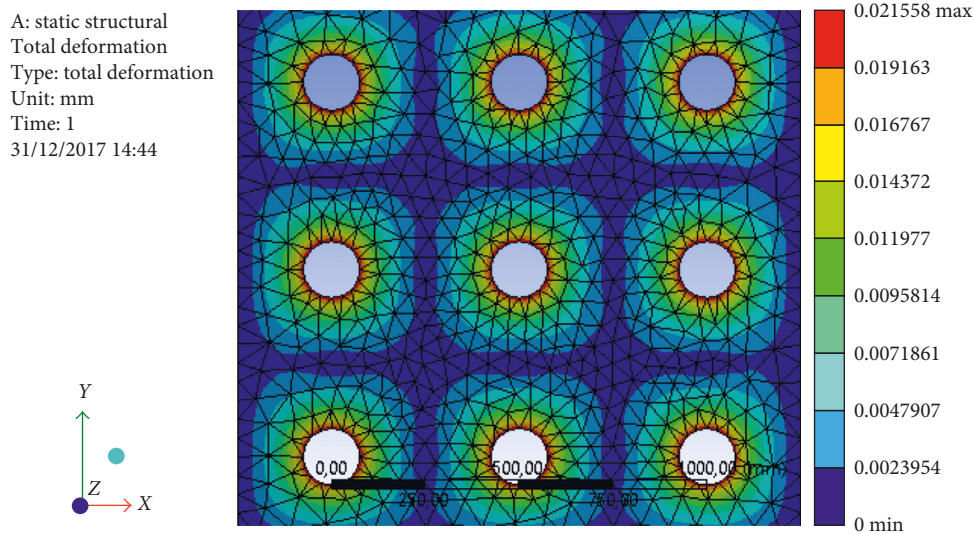


FIGURE 10: Redistribution and magnitude of displacement around 9 holes drilled in the square mesh.

In Figure 8, the portions of the excavation colored blue and red, respectively, represent the areas of compression and tension. The tension zones are smaller than the compression zones. It is therefore concluded that our panel to be filled is generally in a state of compression. The respective maximum stresses are 13,299 MPa and 14,796 MPa. In addition, it is noted that when the spacing hole increases, the intensity of stresses decreases. In Figure 8(a), it is observed that only the normal stresses can create interaction between holes and then could lead to creation of cracks between two holes. This result is in accordance with [7].

Figure 9 presents the maximum value of displacement as the function of spacing holes.

Figure 9 clearly shows that the more the spacing holes increase the more the magnitude of displacements and stresses increase.

3.2.3. Case of Block with Nine Holes Drilled in Square Mesh.

The square mesh distribution of the hole is mostly used in rock quarries. The redistribution and magnitude of stresses and displacement in the case of a block with 9 holes drilled in the square mesh is displayed in Figures 10 and 11.

In Figure 10, the maximum value of displacement is 0.021558 mm. It can be seen that depending on the spacing of holes, there exists interaction between the holes.

In Figures 10 and 11, the parts colored in red and brown represent the zones of tension, while the parts colored in blue represent the zones of compression. The maximum values of the stresses are 13,401 MPa and 13,646 MPa, respectively, for normal stress and shear stress. In Figure 11(a) according to the spacing of holes, the compressive stresses are propagating in the x -direction, while the tensional stresses are propagating in the y -direction. This could allow a controlled fragmentation. However, in Figure 11(b), the

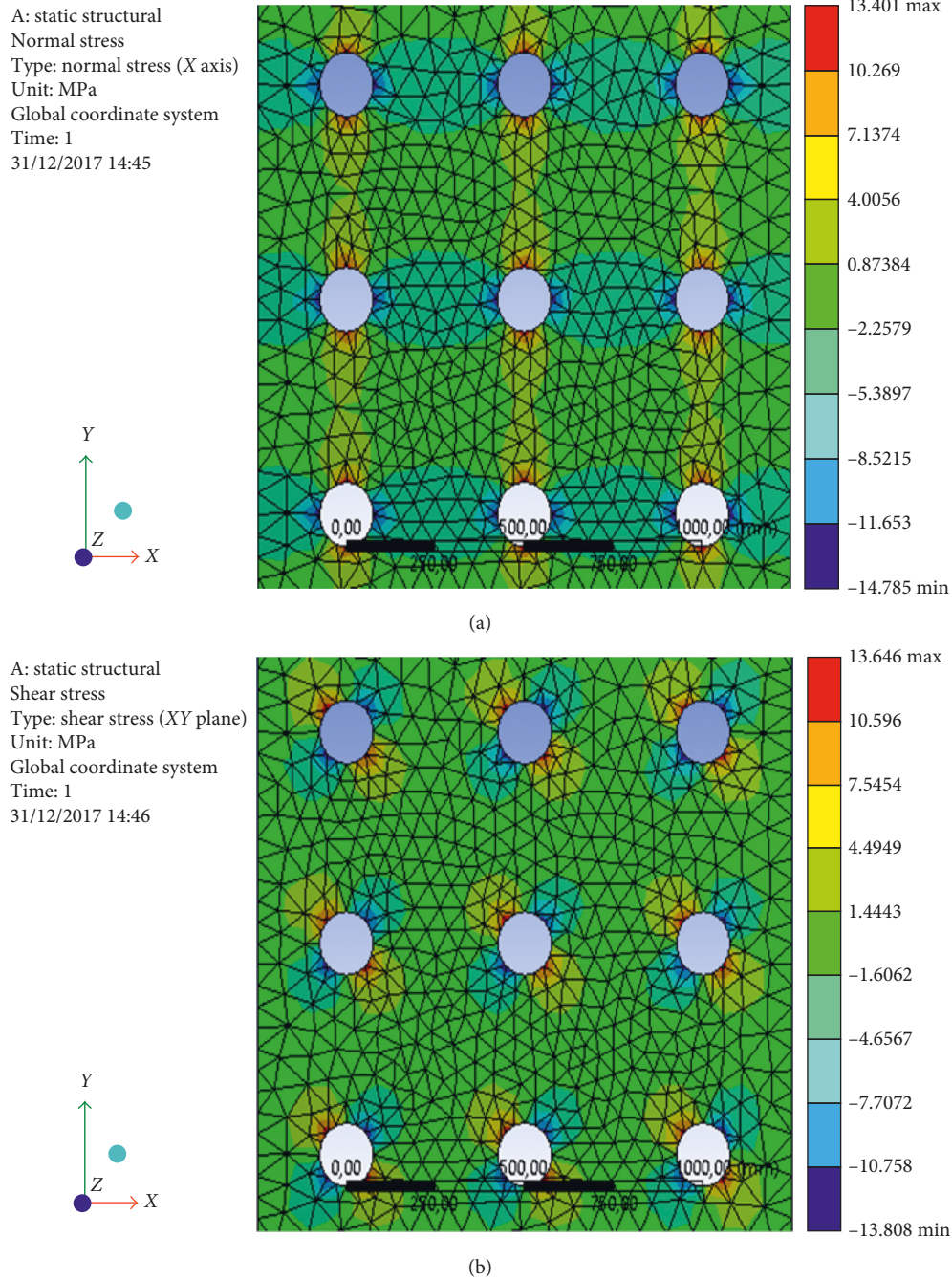


FIGURE 11: Redistribution and magnitude of stresses around 9 holes drilled in the square mesh. (a) Normal stress. (b) Shear stress.

spacing of holes should be very small for in order to allow stress interaction between them.

Figures 12 and 13 show the variations of the stresses and displacements as a function of the distance between the holes of the same line (E) in a square mesh of isotropic elasticity.

Figures 14 and 15 show the variations of stresses and displacement as a function of the distance between the rows (B) of holes in a square mesh.

In Figures 12, 13, 14(b), and 15, it is noted that normal and shear stresses and displacements globally decrease when

the spacing hole increases. For the distance between holes of the same line greater than 48 cm and the distance between the rows of holes greater than 36 cm, stresses seem to be constants. We can conclude that the spacing between the holes of the same line and the spacing between the rows of holes are the important parameters for breaking rock. This result is in accordance with [7].

Engineers should choose suitable spacing hole to control fragmentation. However, in Figure 14(a), the variation of shear stress as a function of the distance between the rows of the hole is more complex.

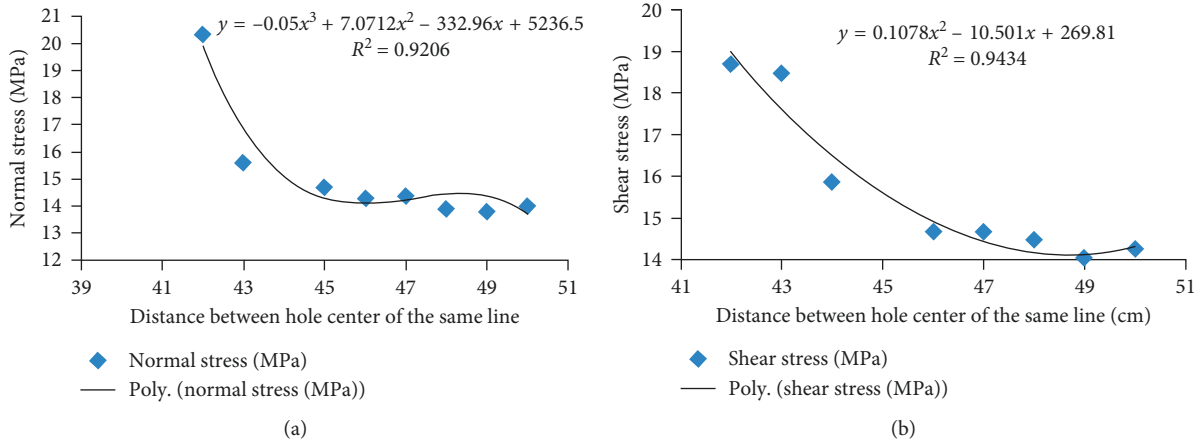


FIGURE 12: (a) Maximum of normal stress and (b) maximum of shear stress as a function of the distance between the holes of the same line in the square mesh.

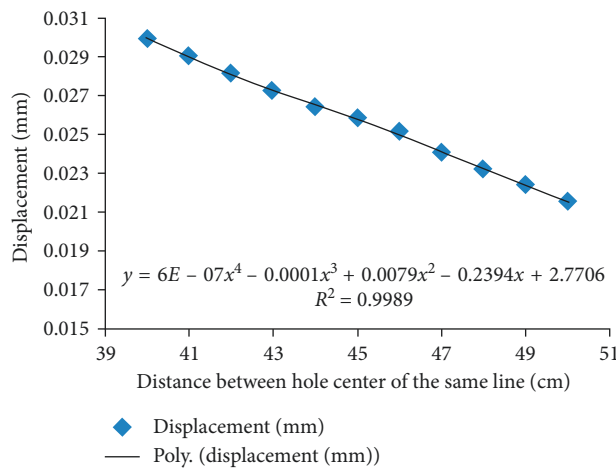


FIGURE 13: Maximum displacement as a function of the distance between the holes of the same line in the square mesh.

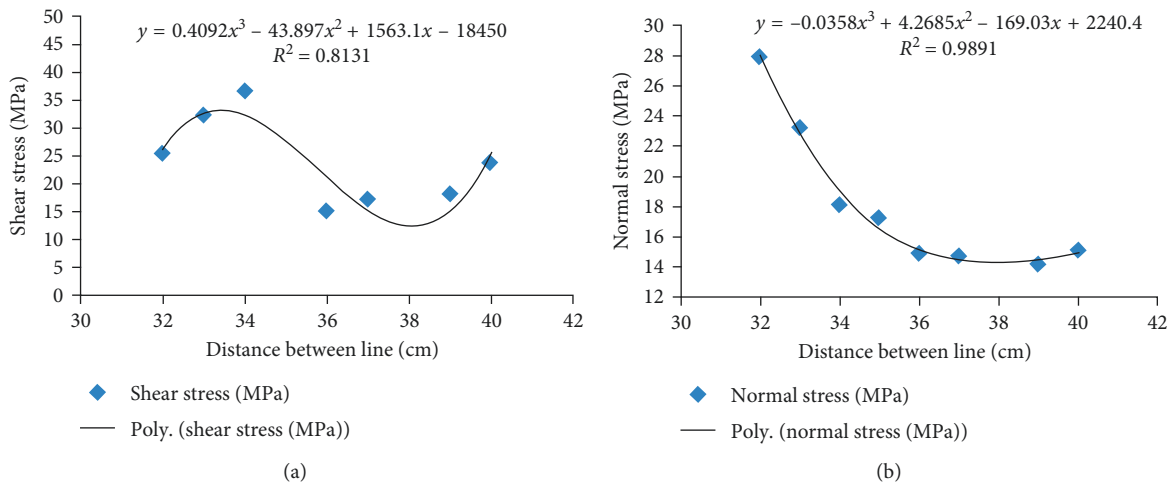


FIGURE 14: (a) Maximum shear stress and (b) maximum normal stress as a function of the distance between the rows of holes drilled in the square mesh.

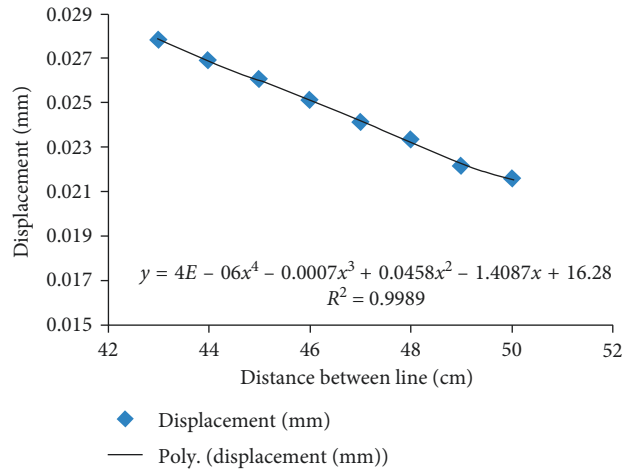


FIGURE 15: Maximum displacement as a function of the distance between the rows of holes in the square mesh.

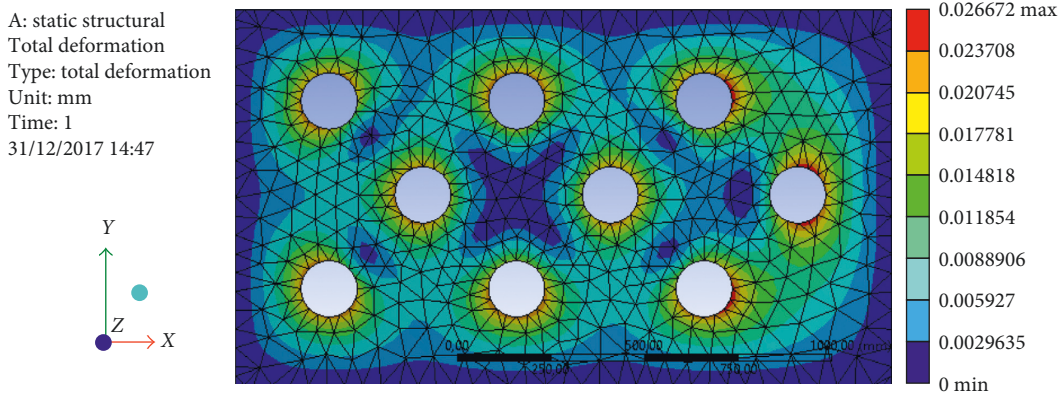
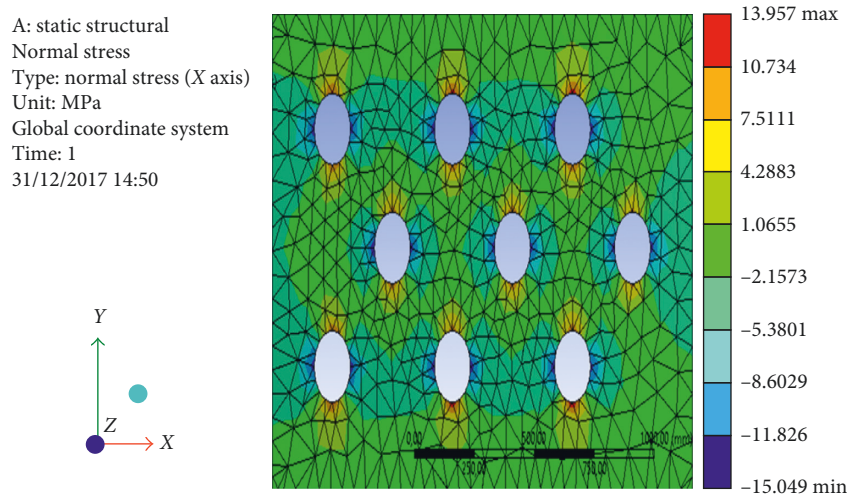


FIGURE 16: Redistribution and magnitude of displacement around 9 holes drilled in the staggered mesh.



(a)

FIGURE 17: Continued.

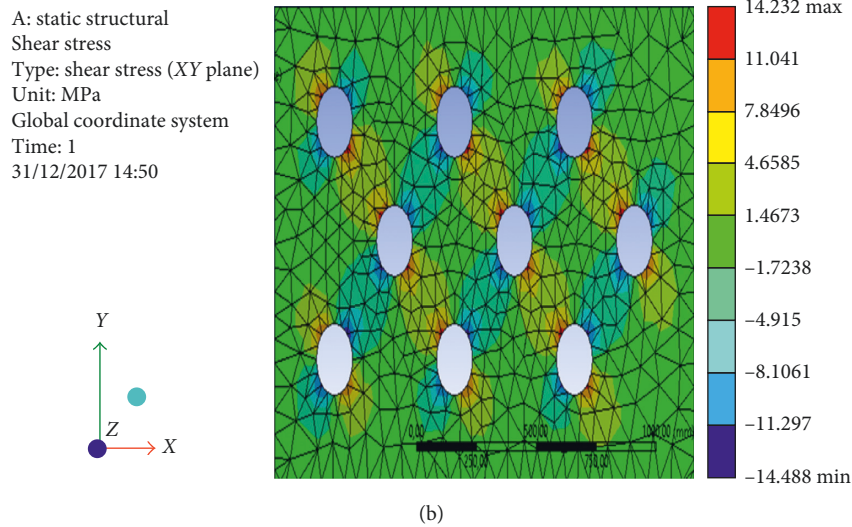


FIGURE 17: Redistribution and magnitude of stresses around 9 holes drilled in staggered mesh. (a) Normal stress. (b) Shear stress.

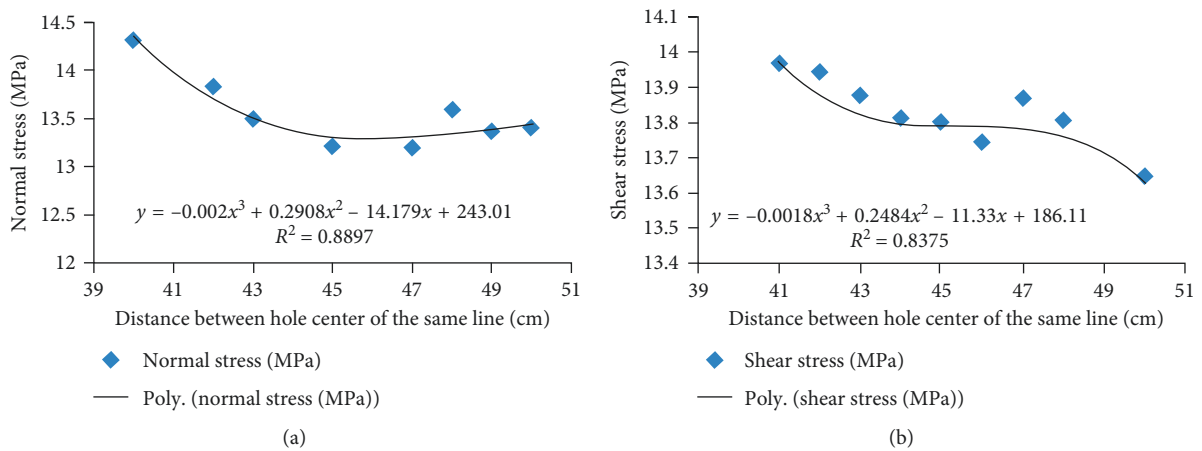


FIGURE 18: Maximum normal stress (a) and shear stress (b) versus distance between holes in the same line in the staggered mesh.

3.2.4. Case of Block with Nine Holes Drilled in Staggered Mesh. Staggered mesh disposition of the hole is mostly used in fragmentation of rocks. Figures 16 and 17 present the redistribution and magnitude of stresses and displacement in the case of a block with 9 holes drilled in the staggered mesh.

In Figure 16, the maximum value of displacement is 0.026672 mm. This value is greater than those obtained in the square mesh disposition of holes. We can observe that, in this type of mesh, the interaction is not only between the holes of the same row but also between the rows.

In Figure 17, the areas colored in red and brown represent the zones of tension, while the parts colored in blue represent the zones of compression. The maximum values of the stresses are 13,957 MPa and 14,232 MPa, respectively, for normal stress and shear stress. These values are greater than those obtained in squares mesh disposition. We can

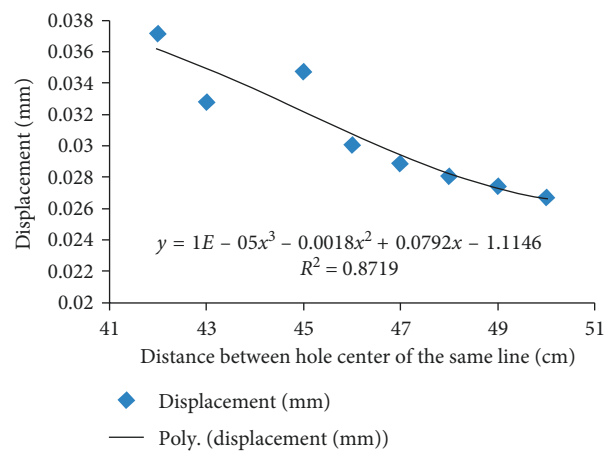


FIGURE 19: Maximum displacement as a function of the distance between the holes of the same line in the staggered mesh.

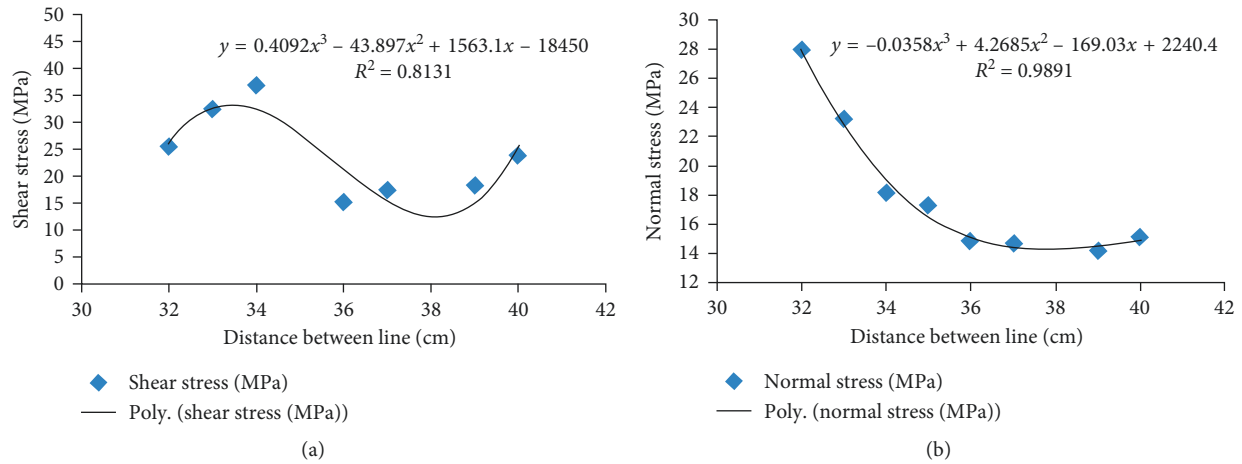


FIGURE 20: Maximum shear stress (a) and maximum normal stress (b) as a function of the distance between the rows of holes in the staggered mesh.

conclude that staggered mesh disposition generates higher stresses than the square mesh disposition. But the square mesh disposition can be useful for a controlled fragmentation in order to obtain block of rock with square geometry. In addition, only the shear stresses (Figure 17(b)) in the staggered disposition allow better stress interaction between holes and then lead to the breaking of rock.

Figures 18 and 19 show the variations of the stresses and deformations as a function of the distance between the holes of the same line in the staggered mesh.

The variations of the stresses and deformations as a function of the distance between the row of holes drilled in the staggered mesh are displayed in Figures 20 and 21.

Figures 18, 19, and 20(b) show that normal and shear stresses and displacements globally decrease when the spacing hole increases. This result is in accordance with [8, 9]. Similar tendency was observed in a square mesh disposition. For the distance between holes of the same line greater than 46 cm and the distance between the rows of holes greater than 38 cm, normal stresses increase slowly. We can conclude that the spacing between the holes of the same line and the spacing between the rows of holes are the important parameters for the breaking of the rock. Engineers should choose suitable spacing hole for controlling fragmentation. However, in Figures 20(a) and 21, the variation of shear stress as a function of the distance between the rows of the hole is more complex. This observation is similar to a square mesh disposition.

4. Conclusion

In this work, we numerically investigated the redistribution of stresses and displacement around holes drilled in a square mesh and a staggered mesh. Numerical results reveal that several factors can influence the mechanical behavior of rocks around the hole: hole diameter, hole spacing, panel mesh, expansive pressure applied, and the elastic properties of the massif, which can be explained as follows:

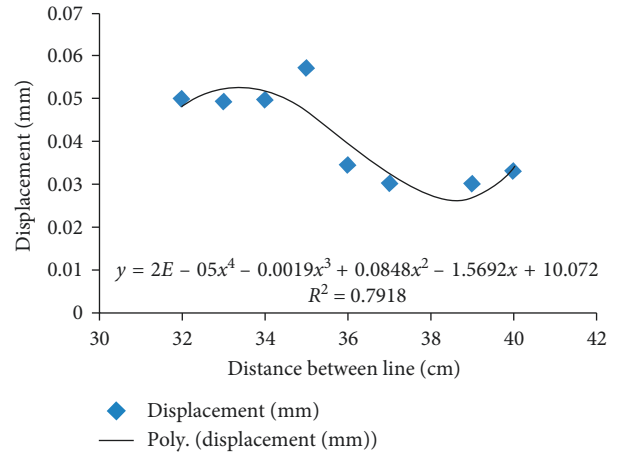


FIGURE 21: Deformation as a function of the distance between rows of holes in the staggered mesh.

- (i) Stresses and displacements globally decrease when spacing holes increase. Similar tendency is observed in [8, 9].
- (ii) Normal stresses allow a better stress interaction between holes in the case of a square mesh disposition.
- (iii) Shear stresses in the staggered disposition allow better stress interaction between holes and then lead to the breaking of the rock. This result is in accordance with [7].
- (iv) For each expansive cement and rock, there exist suitable ranges of diameter of the hole which can generate high stresses.
- (v) For each expansive cement and rock, there exists spacing hole for a controlled fragmentation of rocks.
- (vi) The shear stresses in the staggered disposition allow better stress interaction between holes.

- (vii) The staggered mesh disposition generates higher stresses than the square mesh disposition. But the square mesh disposition can be useful for a controlled fragmentation in order to obtain the block of rock with square geometry.

Data Availability

The data used to support the findings of this study are available from the corresponding author upon request.

Conflicts of Interest

The authors declare that they have no conflicts of interest.

References

- [1] I. Odler, *Special Inorganic Cements*, E&FN Spon, London, UK, 2000.
- [2] S. Timoshenko and J. N. Goodier, *Theory of Elasticity*, McGraw-Hill, New York, NY, USA, 1951.
- [3] A. Musunuri and H. Mitri, "Laboratory investigation into rock fracturing with expansive cement," *International Journal of Mining and Mineral Engineering*, vol. 1, no. 4, 2009.
- [4] S. Torbica and V. Lapcevics, "Rock breakage by explosives," *European International Journal of Science and Technology*, vol. 3, no. 2, 2014.
- [5] C.-H. Ahn and J. W. Hu, "Investigation of key parameters of rock cracking using the expansion of vermiculite materials," *Materials*, vol. 8, no. 10, pp. 6950–6961, 2015.
- [6] E. C. Aifantis, "The physics of plastic deformation," *International Journal of Plasticity*, vol. 3, no. 3, pp. 211–247, 1987.
- [7] E. C. Aifantis, "On the role of gradients on the localization of deformation and fracture," *International Journal of Engineering Science*, vol. 30, no. 10, pp. 1279–1299, 1992.
- [8] I. Mastorakos, L. K. Gallos, and E. C. Aifantis, "Computer simulation of discrete crack propagation," *Journal of the Mechanical Behavior of Materials*, vol. 14, no. 1, 2003.
- [9] G. Efremidis, G. Rambert, and E. C. Aifantis, "Gradient elasticity and size effect for a pressurized thick hollow cylinder," *Journal of the Mechanical Behavior of Materials*, vol. 15, no. 3, 2004.
- [10] E. C. Aifantis, "On stress concentrators and the elimination of elastic singularities: a gradient approach," in *Proceedings of the SEM Annual Conference, Society for Experimental Mechanics Inc.*, Albuquerque, NM, USA, June 2009.
- [11] C. Bagni, H. Askes, and L. Susmel, "Gradient elasticity: a new tool for the multiaxial high-cycle fatigue assessment of notched components," in *Proceedings of Annual Postgraduate Research Student Conference*, Sheffield, UK, 2016.
- [12] E. C. Aifantis, "Internal length gradient (ILG) mechanics across scales and disciplines," *Advances in Applied Mechanics*, vol. 49, pp. 1–110, 2016.
- [13] S. Arshadnejad, K. Goshtasbi, and J. Aghazadeh, "Stress concentration analysis between two neighboring circular holes under internal pressure of a non-explosive expansion material," *Journal of the Earth Sciences Application and Research Centre of Hacettepe University*, vol. 30, no. 3, pp. 261–262, 2009.
- [14] S. Arshadnejad, K. Goshtasbi, and J. Aghazadeh, "A model to determine hole spacing in the rock fracture process by non-explosive expansion material," *International Journal of Minerals, Metallurgy and Materials*, vol. 18, no. 5, pp. 509–514, 2011.
- [15] R. Sburlati, "Analytical elastic solutions for pressurized hollow cylinders with internal functionally graded coatings," *Composite Structures*, vol. 94, no. 12, pp. 3592–3600, 2012.
- [16] W. Shen, Y. Yu, X. Wang, J. Bai, and W. Li, "Rock stress around noncircular tunnel: a new simple mathematical method," *Advances in Applied Mathematics and Mechanics*, vol. 9, no. 6, pp. 1330–1346, 2017.
- [17] E. R. A. Nkene, M. N. L. Leroy, N. Joseph, D. E. Sandring, and N. Jean-Marie Bienvenu, "Displacements, strain and stress investigations in an inhomogeneous rotating hollow cylinder made of functionally graded materials under an axisymmetric radial loading," *World Journal of Mechanics*, vol. 8, no. 3, pp. 59–72, 2018.
- [18] O. C. Zienkiewicz, *The Finite Element Method in Engineering Science*, McGraw-Hill, New York, NY, USA, 1971.
- [19] C. S. Accensi, *Advanced of Notions of Rock Mechanics: Confrontation of Mechanical and Geological Models with the Reality of a Construction Site of the Digging of a Tunnel in a Fractured Rock Mass*, Mining School of Alès, Alès, France, 2011.
- [20] C. Frey, "Modeling of physical properties and elasticity by the finite element method," Master's thesis, Department of Electrical and Computer Engineering, Faculty of Science and Naval Engineering, University of Laval, Canada, 1999.
- [21] S. G. Lekhnitskii, *Theory of Elasticity of an Anisotropic Elastic Body*, Holden Day, San Francisco, CA, USA, 1963.
- [22] M. N. L. Leroy, N. Joseph, and N. J. Marie, "Redistribution and magnitude of stresses and strains around horse shoe and circular excavations opened in anisotropic rock," *International Journal of Mining Science and Technology*, vol. 25, no. 4, pp. 615–621, 2015.

